NOTES AND CORRESPONDENCE

On the Radiative and Dynamical Feedbacks over the Equatorial Pacific Cold Tongue

DE-ZHENG SUN

NOAA–CIRES Climate Diagnostics Center, Boulder, Colorado

JOHN FASULLO

Program in Atmospheric and Oceanic Sciences, University of Colorado, Boulder, Colorado

TAO ZHANG AND ANDRES ROUBICEK

NOAA–CIRES Climate Diagnostics Center, Boulder, Colorado

2 May 2002 and 5 February 2003

ABSTRACT

An analysis of the climatic feedbacks in the NCAR Community Climate Model, version 3 (CCM3) over the equatorial Pacific cold tongue is presented. Using interannual signals in the underlying SST, the radiative and dynamical feedbacks have been calculated using both observations and outputs from the NCAR CCM3. The results show that the positive feedback from the greenhouse effect of water vapor in the model largely agrees with that from observations. The dynamical feedback from the atmospheric transport in the model is also comparable to that from observations. However, the negative feedback from the solar forcing of clouds in the model is significantly weaker than the observed, while the positive feedback from the greenhouse effect of clouds is significantly larger. Consequently, the net atmospheric feedback in the CCM3 over the equatorial cold tongue region is strongly positive (5.1 W m^{-2} K^{-1}), while the net atmospheric feedback in the real atmosphere is strongly negative (-6.4 W m^{-2} K^{-1}). A further analysis with the aid of the International Satellite Cloud Climatology Project (ISCCP) data suggests that cloud cover response to changes in the SST may be a significant error source for the cloud feedbacks. It is also noted that the surface heating over the cold tongue in CCM3 is considerably weaker than in observations. In light of results from a linear feedback system, as well as those from a more sophisticated coupled model, it is suggested that the discrepancy in the net atmospheric feedback may have contributed significantly to the cold bias in the equatorial Pacific in the NCAR Climate System Model (CSM).

1. Introduction

The sensitivity of the climate system to an external perturbation depends critically on the feedbacks in the climate system (Manabe and Wetherald 1967; Sun and Lindzen 1993; Houghton et al. 2001). For the same reason that feedbacks affect the climate sensitivity to an external perturbation, one expects that feedbacks may play an important role in determining the amplitude of natural variability. The recent study by Hall and Manabe (1999) on the role of water vapor in determining the amplitude of low-frequency variability has provided a concrete example. A less studied topic is the role of the feedbacks in determining the equilibrium state of the climate system or the time-mean climate. On theoretical grounds, one expects that the equilibrium state of the climate system may also depend strongly on how the subcomponents communicate (i.e., how they respond to each other's signal) and therefore on the feedbacks. This issue is more visible in the area of coupled climate modeling. Why do coupled models often settle to climates that in some aspects are quite different from the observed even though the individual components run with the observed boundary conditions simulate the observed climate well? One possible answer to this question is that coupling invokes the effect of feedback processes. In this note we will provide a specific example to illustrate how errors in the feedbacks in the National Center for Atmospheric Research (NCAR) Community Climate Model (CCM3; Kiehl et al. 1998)—the atmospheric component of the NCAR Climate System Model (CSM; Boville and Gent 1998)—may have significantly contributed to the development of an excessive cold tongue in the equatorial Pacific in the model. As first reported in Boville and Gent (1998) and Kiehl (1998), the equatorial Pacific SST is considerably colder in the NCAR CSM than in observations.

Corresponding author address: Dr. De-Zheng Sun, NOAA–CIRES Climate Diagnostics Center, 325 Broadway, Boulder, CO 80309-0449.
E-mail: ds@cdc.noaa.gov

With the cold tongue problem in mind, we focus our initial analysis of the atmospheric feedbacks on the region of the tropical Pacific—the feedbacks over the equatorial Pacific cold tongue region, in particular. There are additional reasons to focus on this region. First, to quantify feedbacks, one needs a sufficiently large signal in the SST field. El Niño warming in the equatorial Pacific provides such a signal. Also, better at simulating the tropical Pacific climate, the El Niño–Southern Oscillation (ENSO) phenomenon, in particular, has been a priority of current modeling activities involving the use of fully coupled GCMs including the NCAR CSM (Latif et al. 2001).

Previous feedback analysis has largely focused on radiative processes involving water vapor and clouds (Cess et al. 1990; Sun and Held 1996; and many others). Quantification of the corresponding dynamical feedback has been largely ignored. Here the purpose is to identify the feedbacks that are mostly different from observations with an eye to better understand the causes of the excessive cold tongue in the NCAR CSM. We therefore calculate the radiative as well as the dynamical feedbacks—a process that has been made possible by the work of the NCAR climate analysis section in calculating atmospheric transports (Trenberth 1997; Trenberth et al. 2001). By combining the radiative fluxes at the top of the atmosphere (TOA) from the Earth Radiation Budget Experiment (ERBE; Barkstrom et al. 1989) with the atmospheric transport, one can obtain the net atmospheric feedback and also the net surface heat flux into the ocean.

Our methodology is very simple—we will examine how radiative fluxes at TOA and the vertically integrated transport of energy in the atmosphere vary in relation to the underlying SST. We quantify the feedbacks by regressing the corresponding flux to the SST. Figure 1 schematically illustrates the physical processes and the corresponding feedbacks we will quantify and report in this note.

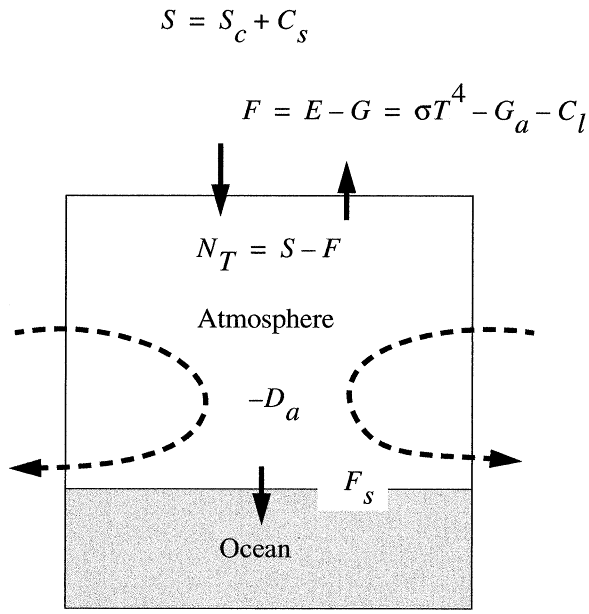

FIG. 1. A schematic diagram illustrating the physical processes and the corresponding atmospheric feedbacks over the cold tongue region. Here S and F are, respectively, the net solar radiation received at the TOA and the outgoing longwave radiation at the TOA; S_c and C_s are, respectively, the clear-sky solar radiation and the shortwave forcing of clouds (Ramanathan and Collins 1991); E is the surface emission; G is the total greenhouse effect; G_a and C_l are, respectively, the greenhouse effect of water vapor and clouds; N_T is the net radiative flux at the top of the atmosphere; D_a is the vertically integrated, horizontal convergence of total energy in the atmosphere; F_s is the net surface heat flux into the ocean. The atmospheric circulation over the cold tongue region is characterized by divergence in the lower troposphere and convergence in the upper troposphere.

2. Results

The SST signal averaged over the equatorial cold tongue (5°S–5°N, 160°–290°E) is shown in Fig. 2a. It includes the 1986/87 El Niño warming as well as the 1988/89 La Niña cooling. The responses of the greenhouse effect of water vapor (G_a), the vertically integrated horizontal convergence of total atmospheric energy (D_a), the greenhouse effect of clouds (C_l), the shortwave forcing of clouds (C_s), and the latter two combined ($C_l + C_s$), averaged over the cold tongue region to the SST signal are shown, respectively, in Figs. 2b,c,d,e,f. Presented are their interannual anomalies over the period of ERBE. The radiative fluxes are from ERBE (Barkstrom et al. 1989). The data for the atmospheric divergence of energy are the same as that used in Sun and Trenberth (1998; see also Trenberth et al. 2001). The model data are from a run of CCM3 with the observed monthly varying SST. Therefore the model and the real atmosphere have the same SST forcing. CCM3 is a global spectrum model. It has a horizontal T42 resolution and 18 levels in the vertical. Deep convection is parameterized using the scheme of Zhang and McFarlane (1995) and shallow convection is parameterized by the scheme of Hack (1994). Detailed description of CCM3 can be found in Kiehl et al. (1998).

The response of the greenhouse effect of water vapor from the model appears to largely agree with that from observations (Fig. 2b). The overestimate in the model appears to be small relative to the total response. The response of the horizontal transport by atmospheric circulations is also very comparable to observations (Fig. 2c). More substantial differences are found in the cloud feedbacks. Figures 2d,e show, respectively, the variations of shortwave (thin line) and longwave (thick line) over the ERBE period and the corresponding results from the model simulations. Observations show a strong negative feedback from the solar forcing of clouds. This feedback has the correct sign in the model simulations, but its strength is substantially underestimated (Figs. 2d,e). The model also significantly overestimates the positive response of the greenhouse effect of clouds. Consequently, while the greenhouse effect of clouds

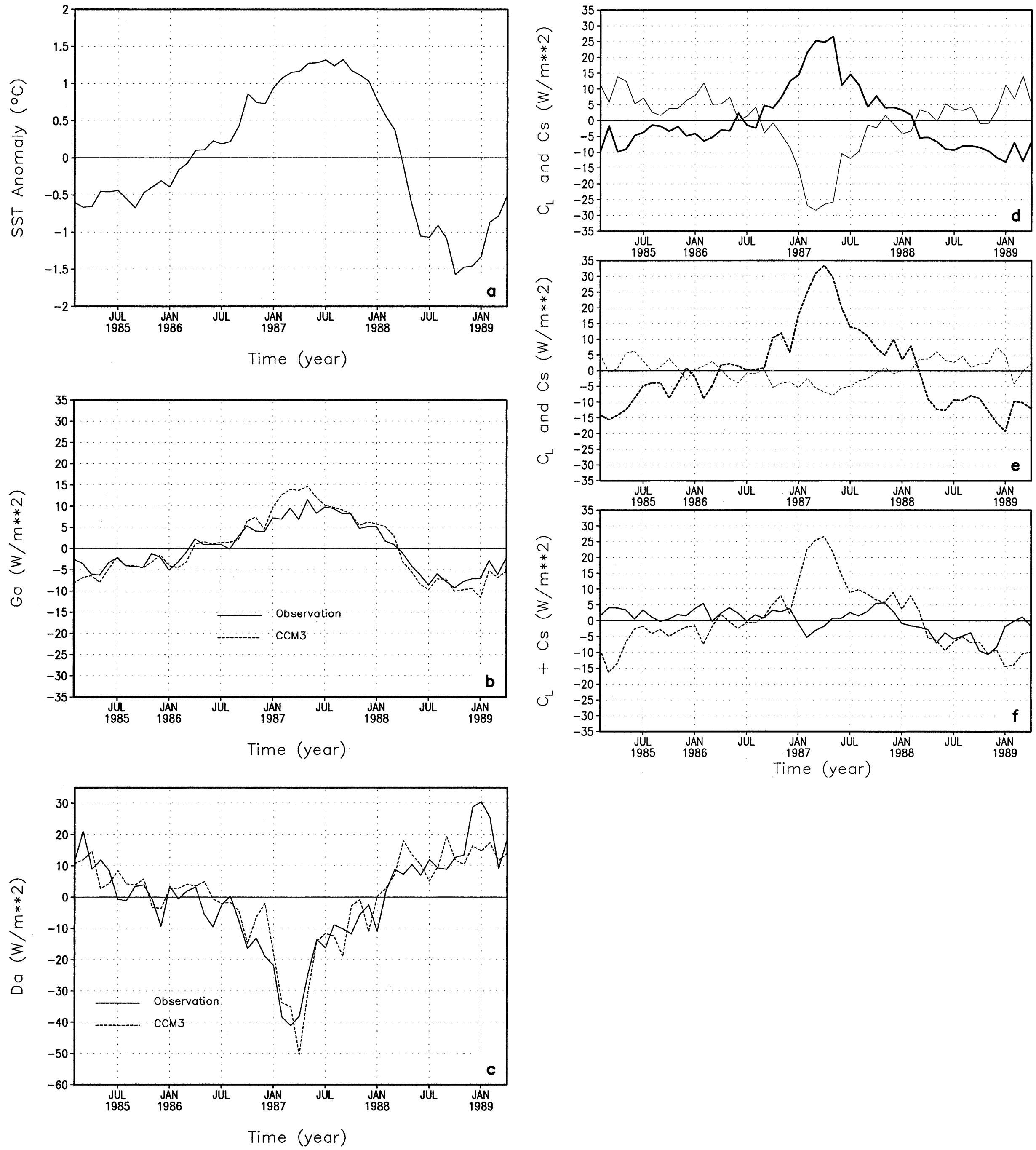

FIG. 2. (a) The SST signal. (b) Response of the greenhouse effect of water vapor (G_a) to the SST signal in observations (solid line) and in the CCM3 (dashed line). (c) Response of D_a to the SST signal in ERBE observations (solid line) and in the CCM3 (dashed line). (d) Response of C_l (thin solid line) and C_s (thick solid line) to the SST signal in observations. (e) Response of C_l (thick dashed line) and C_s (thin dashed line) to the SST signal in CCM3 (dashed line). (f) Response of $C_l + C_s$ to the SST signal in observations (solid line) and in the CCM3 (dashed line). Shown are interannual anomalies of the corresponding quantities in the equatorial cold tongue region (5°S–5°N, 160°–290°E) over the ERBE period.

cancels well with the shortwave forcing of clouds in nature, the greenhouse effect of clouds in the model far outweighs the shortwave forcing of clouds (Fig. 2f). The lack of cancellation in the model was noted earlier by Kiehl et al. (1998) by regressing C_l to C_s using their spatial and temporal variations, but it is now clearer that errors in both C_l and C_s contribute significantly to the larger ratio of C_l over C_s in the model. It is interesting

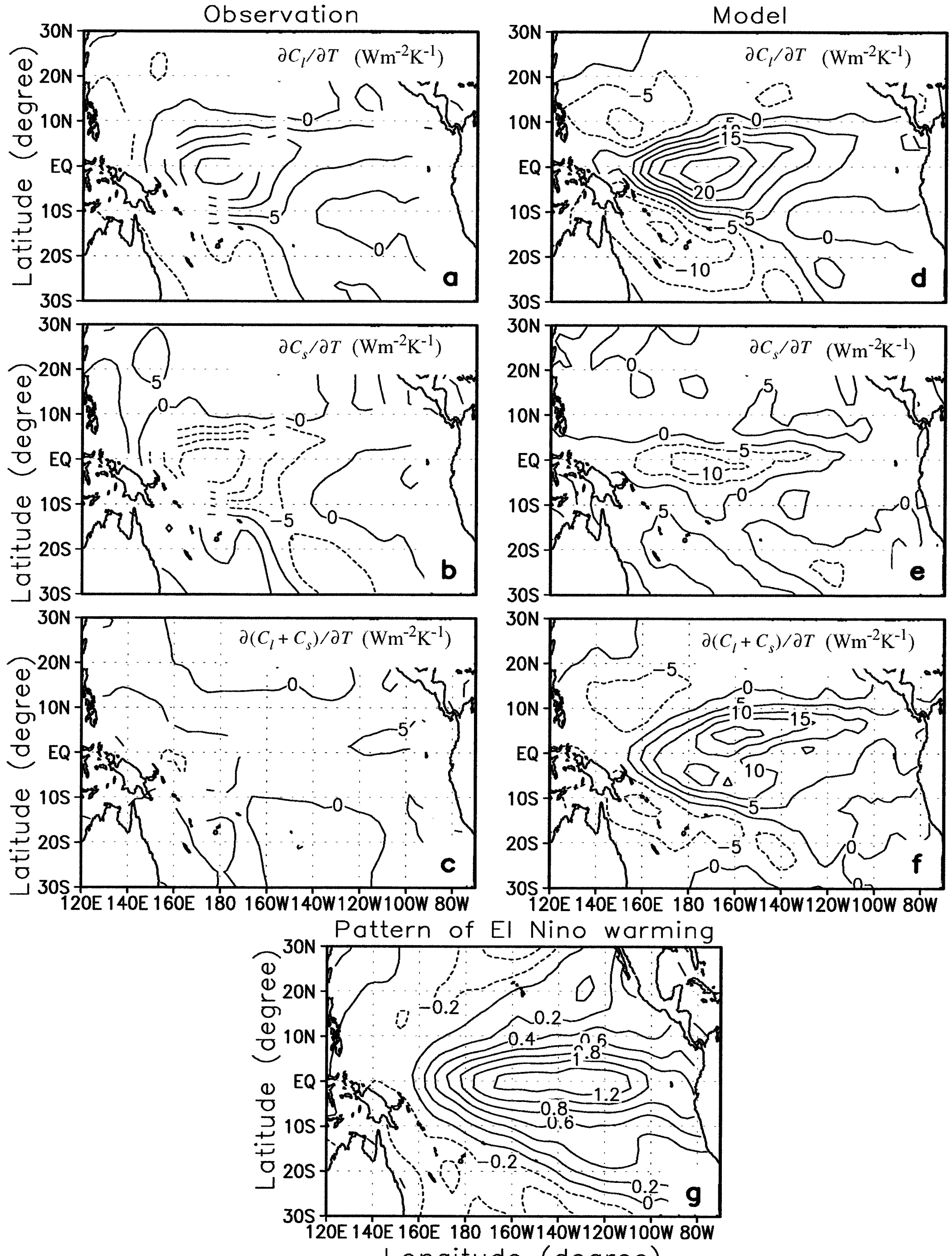

FIG. 3. Spatial pattern of the response in C_l, C_s, and $C_l + C_s$ to El Niño warming in the (a), (b), (c) observations and in (d), (e), (f) the CCM3 simulations. The spatial pattern of the El Niño warming is also shown. (g) Linear regressions of C_l, C_s, $C_l + C_s$, and SST to the cold tongue SST index shown in Fig. 2a. (It is therefore explicitly assumed that the response to La Niña cooling is a mirror image of the response to El Niño warming.)

to note that the spatial pattern of the response of C_l and C_s in the model is in fact quite realistic. The responses in the model are just of the wrong amplitude (Fig. 3). Consistent with the stronger feedback from C_l and the weaker feedback from C_s in the model, the response in the upper-level cloud cover to SST warming is found to be larger in the model than in observations while the response in the cloud cover at lower levels is found to be weaker (Fig. 4).

Since the storage term in the atmosphere is small, the

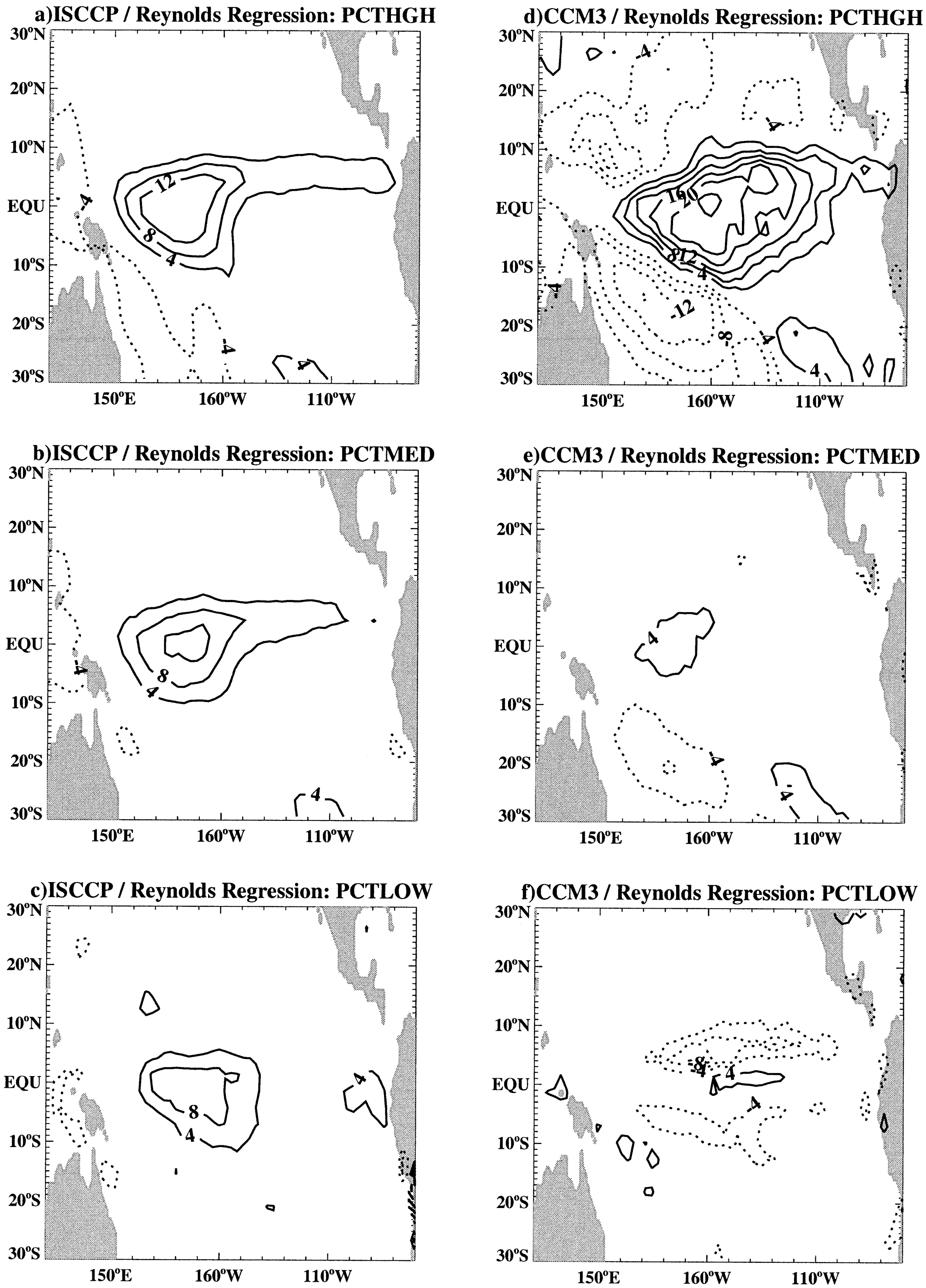

FIG. 4. Response of the upper, middle, and low cloud cover to El Niño warming in (a), (b), (c) observations and in (d), (e), (f) CCM3 simulations. Shown are linear regressions of the cloud covers to the cold-tongue SST index shown in Fig. 2a. The observational results were obtained using the data from ISCCP (Rossow et al. 1996; Rossow and Schiffer 1999). The levels used to define low-, mid-, and upper-level clouds in ISCCP data are 680, 440, and 50 mb, which differ slightly from the corresponding levels used in the model data (700, 400, and 50 mb). Despite the slightly narrower slab used in CCM3 for calculating high cloud cover, the response of the upper cloud cover in the model is much stronger. In obtaining the mid and low cloud level, ISCCP cloud cover has been adjusted for cloud layering assuming a random cloud overlap. Thus the differences in mid- and low-level cloud cover response between CCM3 and ISCCP are less certain quantitatively than the differences in the upper-level clouds.

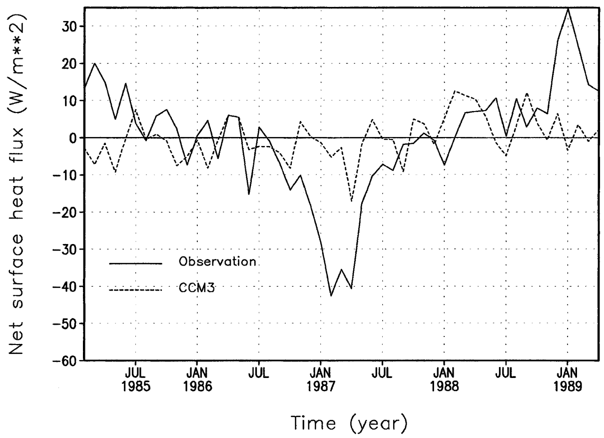

FIG. 5. Variations of the net surface heat flux over the equatorial cold tongue region (5°S–5°N, 160°–290°E) in observations (solid line) and in the NCAR CCM3 (dashed line).

errors in the above feedbacks are well reflected in the net surface heat flux into the ocean (Fig. 5). A more quantitative measure of the various feedbacks may be obtained by linearly regressing the variations of the corresponding quantities to the SST variations. This is equivalent to approximating the atmosphere over the cold tongue region as a linear feedback system. The results are summarized in Table 1. The numbers confirm the impression that largely due to the errors in the clouds, the net atmospheric feedback in the model is strongly positive while the net atmospheric feedback in the real atmosphere is estimated to be strongly negative (for reference, recall that the rate of blackbody emission at 300 K is about 6.1 W m^{-2} K^{-1}). The table also shows that the model significantly overestimates the feedback from the greenhouse effect of water vapor. In terms of the feedback from the net surface heat flux into the ocean, the strong net negative feedback from the real atmosphere implies that a drift in SST from a reference state will be strongly constrained by the atmosphere. This constraining effect barely exists in the model atmosphere.

A quantitative measure of the effect of a more positive net atmospheric feedback on the equilibrium SST of the coupled model over the equatorial Pacific may be obtained by approximating the coupled ocean–atmosphere system over that region as a linear feedback system. For such a system, the equilibrium SST may be written as

$$T = T_0 + \frac{H(T_0)}{4\sigma T_0^3 - \left(\frac{\partial G_a}{\partial T} + \frac{\partial C_l}{\partial T} + \frac{\partial C_s}{\partial T} + \frac{\partial D_a}{\partial T}\right) - \frac{\partial D_o}{\partial T}}, \tag{1}$$

where T is the equilibrium SST, T_0 is the observed SST of the cold tongue (5°S–5°N, 160°–290°E), and σ is the Stefan–Boltzman constant. Here $\partial G_a/\partial T$, $\partial C_l/\partial T$, $\partial C_s/\partial T$, $\partial D_a/\partial T$ are, respectively, the feedbacks from the greenhouse effect of water vapor, the greenhouse effect of

TABLE 1. Atmospheric feedbacks over the equatorial Pacific cold tongue region (5°S–5°N, 160°–290°E) from observations and the CCM3 simulations. They are obtained through a linear regression using the SST signal (Fig. 2a) and the interannual variations of the corresponding fluxes over the cold tongue region. Here $\partial F_A/\partial T$ is the net atmospheric feedback.

	Feedback (W m^{-2} K^{-1})	
Name of process	Observations	Model
$\frac{\partial(G_a)}{\partial T}$	6.37 ± 0.23	8.26 ± 0.33
$\frac{\partial(C_L)}{\partial T}$	9.81 ± 0.88	12.96 ± 1.02
$\frac{\partial(C_S)}{\partial T}$	−7.79 ± 1.23	−2.98 ± 0.43
$\frac{\partial(D_a)}{\partial T}$	−14.80 ± 1.47	−13.18 ± 1.48
$\frac{\partial(F_A)^*}{\partial T}$	−6.41 ± 1.69	5.06 ± 0.96
$\frac{\partial(F_S)}{\partial T}$	−12.73 ± 1.72	−0.91 ± 0.96
$\frac{\partial(N_T)}{\partial T}$	2.37 ± 0.56	12.27 ± 1.12

* The net atmospheric feedback is $\partial(F_A)/\partial T = \partial(G_a)/\partial T + \partial(C_L)/\partial T + \partial(C_S)/\partial T + \partial(D_a)/\partial T$.

clouds, the shortwave forcing of clouds, and the transport by the atmospheric circulations; $\partial D_o/\partial T$ is the feedback from the ocean transport; and $H(T_0)$ is the net heating that the coupled model is subject to at the observed SST. If the model components are perfect, $H(T_0)$ is zero. Equation (1) is obtained by expanding the total energy equation of the coupled model over the cold tongue region about the observed SST. Figure 6 shows the dependence of a cold bias in the equilibrium SST on the net atmospheric feedback. In this calculation, the coupled ocean–atmosphere over the cold tongue region is assumed to be subject to a cooling at the observed SST (T_0). The magnitude of this cooling [$H(T_0)$] is estimated from biases in the surface heat flux over the cold tongue region in the CCM3 run with the observed SST as the boundary conditions. Figure 6 shows that the magnitude of the cold bias is only 0.5°C if the model atmosphere has the same feedbacks as the real atmosphere. The cold bias, however, is amplified to 1.0°C when the atmospheric model has the same feedbacks as those in CCM3. The difference is even larger if a less negative ocean feedback is used (dashed line in the figure). In order to calculate the ocean feedback explicitly, we have further inserted a linear feedback atmosphere to the coupled model of Sun (2003) over the equatorial cold tongue region (5°S–5°N, 160°–290°E). The surface heat flux into the ocean over this

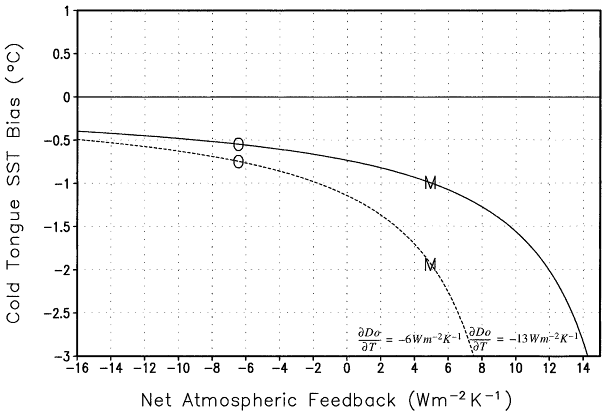

FIG. 6. Cold biases in the equilibrium SST as a function of the net atmospheric feedback. The coupled ocean–atmosphere over the cold tongue region (5°S–5°N, 160°–290°E) is approximated as a linear feedback system (see text for more details). In the calculation, we choose $T_0 = 300$ K and $H(T_0) = -13.8$ W m^{-2}. The value for $H(T_0)$ here is taken as the difference between the net surface heat flux over the cold tongue region in CCM3 run with observed SST and the net surface heat flux estimated from observations (see Fig. 8). This is equivalent to assuming that the ocean component run with observed surface forcing gives the correct ocean transport. The ''O'' marks the equilibrium cold bias if the atmospheric model has the same net atmospheric feedback as the real atmosphere. The ''M'' marks the equilibrium cold biases when the atmosphere has the same net atmospheric feedback as the CCM3.

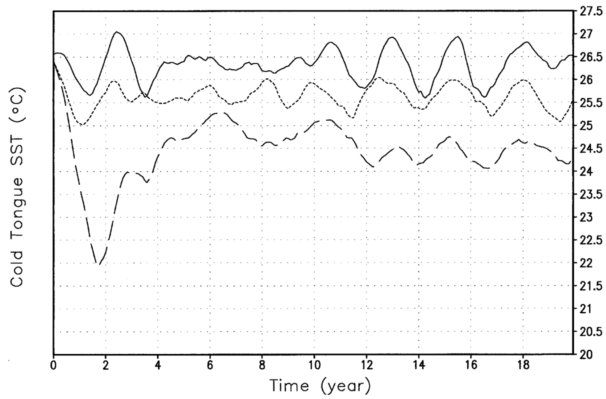

FIG. 7. Time series of the cold tongue SST from a control run (solid line) and two cooling experiments (dashed lines) from a modified version of Sun (2003). The model is essentially the same as Sun (2003) except with a linear feedback atmosphere being inserted to the model over the equatorial cold tongue region (5°S–5°N, 160°–290°E) [see Eq. (2) in the main text]. The first cooling experiment has the observed atmospheric feedbacks (short dashed line). The second cooling experiment has the feedbacks from the CCM3 (long dashed line). The cooling is a reduction in F_{s0} of 13.8 W m^{-2}, uniformly applied to the equatorial cold-tongue region. The equatorial surface wind is coupled with the zonal SST contrast in the same way as in Sun (2003).

region (F_s) at a given SST is then given by the following equation:

$$F_s = F_{s0} - \left[4\sigma T_0^3 - \left(\frac{\partial G_a}{\partial T} + \frac{\partial C_l}{\partial T} + \frac{\partial C_s}{\partial T} + \frac{\partial D_a}{\partial T}\right)\right] \times (T - T_0), \tag{2}$$

where T_0 is the observed SST, F_{s0} is the surface heat flux at T_0, and T is the SST. Equation (2) is obtained by linearizing the energy balance equation for the atmosphere about the observed SST (T_0). When the coupled ocean–atmosphere reaches an equilibrium,

$$F_s + D_0 = 0, \tag{3}$$

where D_o represents the heating due to ocean transport. It is now calculated by the coupled model instead of being assumed to be a linear function of T. [When the ocean is also approximated by a linear feedback system, Eqs. (2) and (3) are reduced to Eq. (1).] Three experiments have been conducted: a control run and two perturbed runs with, respectively, the observed and the modeled atmospheric feedbacks. The perturbation is an initial cooling over the cold tongue region—a reduction in F_{s0}. Figure 7 shows the time series of cold tongue SST from these experiments. Again, the experiment with the feedbacks from CCM3 settles to a colder state.

The assumption that the coupled ocean–atmosphere is subject to an initial cooling with the observed SST is valid, as the surface heat flux in the CCM3 run with observed SST is considerably weaker than that from observations (Fig. 8). A full diagnosis of the causes for the deficiencies in the net surface heat flux is beyond the scope of the present paper. Note that the effect of the atmospheric feedbacks on the development of the

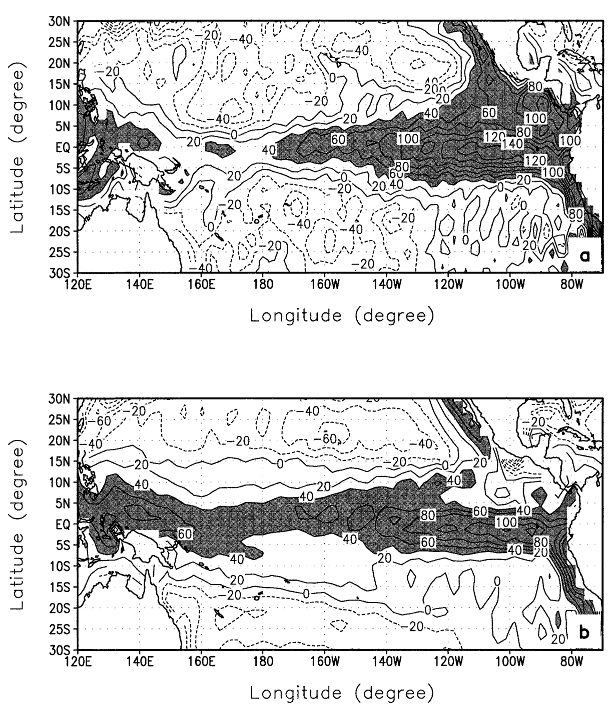

FIG. 8. Long-term mean net surface heat flux over the Pacific in (a) observations and in the (b) NCAR CCM3. The observational data are from Trenberth et al. (2001).

cold bias in the coupled model is independent of whether the initial cooling error comes from the atmosphere or the ocean.

3. Summary

Using interannual signals in tropical SST, the radiative and dynamical feedbacks in the tropical atmosphere have been calculated using both observations and outputs from the NCAR CCM3. The results show that the net atmospheric feedback in the CCM3 over the equatorial Pacific cold tongue region is strongly positive (5.1 $W\ m^{-2}\ K^{-1}$), while the net atmospheric feedback in the real atmosphere is strongly negative ($-6.4\ W\ m^{-2}\ K^{-1}$). This discrepancy is largely due to errors in cloud feedbacks—the positive feedback from the greenhouse effect of clouds in the model is significantly larger than the observed, while the negative feedback from the solar forcing of clouds in the model is significantly weaker. Further noting a weaker surface heating over the cold tongue in the CCM3 than in observations, and in light of some model results, we suggest that the discrepancy in the net atmospheric feedbacks may have contributed significantly to the cold bias in the equatorial Pacific (the excessive equatorial Pacific cold tongue) in the NCAR CSM.

A further analysis with the aid of the International Satellite Cloud Climatology Project (ISCCP) data suggests that the apparent errors in the cloud feedbacks may be in part due to errors in the cloud cover response to changes in the SST. For a more complete diagnosis of the error sources, cloud optical properties need also be compared with observations. Unfortunately, the present standard outputs from CCM3 do not appear to permit a direct comparison of the upper- and low-level cloud water/ice content in the model with ISCCP observations. More work also needs to be done to understand why the CCM3 underestimates the surface heat flux into the equatorial cold tongue. Outputs from the newly modified Community Climate Atmospheric Model (CAM) and the corresponding coupled runs will provide further opportunities to address issues raised in this study.

Acknowledgments. This research was supported partially by the NSF Climate Dynamics Program (ATM-9912434) and partially by NOAA's Office of Global Programs [the Climate Dynamics and Experimental Prediction Program, the Climate Variability and Predictability (CLIVAR)/PACS Program, and the CLIVAR/Pacific Program]. The leading author (D.-Z. Sun) would like to thank Drs. William Collins, James Hack, Jeff Kiehl, Steve Klein, and Isaac Held for the helpful discussions. D.-Z. Sun would also like to thank the three anonymous reviewers for their insightful comments and Dr. Leo Donner for his editorial efforts.

REFERENCES

Barkstrom, B. R., E. F. Harrison, G. L. Smith, R. Green, J. Kibler, R. D. Cess, and the ERBE Science Team,1989: Earth Radiation Budget Experiment (ERBE) Archival and April 1985 Results. *Bull. Amer. Meteor. Soc.,* **70,** 1254–1262.

Boville, B., and P. Gent, 1998: The NCAR Climate System Model, version one. *J. Climate,* **11,** 1115–1130.

Cess, R. D., and Coauthors, 1990: Intercomparison and interpretation of climate feedback processes in 19 atmospheric circulation models. *J. Geophys. Res.,* **95,** 16 601–16 615.

Hack, J. J., 1994: Parameterization of moist convection in the National Center for Atmospheric Research Community Climate Model (CCM2). *J. Geophys. Res.,* **99,** 5551–5568.

Hall, A., and S. Manabe, 1999: The role of water vapor feedback in unperturbed climate variability and global warming. *J. Climate,* **12,** 2327–2346.

Houghton, J. T., Y. Ding, D. J. Griggs, M. Noguer, P. J. van der Linden, X. Dai, K. Maskel, and C. A. Johnson, Eds., 2001: *Climate Change 2001*: *The Scientific Basis.* Cambridge University Press, 881 pp.

Kiehl, J. T., 1998: Simulation of the tropical Pacific warm-pool with the NCAR climate system model. *J. Climate,* **11,** 1342–1355.

——, J. J. Hack, G. Bonan, B. A. Boville, D. Williamson, and P. J. Rasch, 1998: The National Center for Atmospheric Research Community Climate Model: CCM3. *J. Climate,* **11,** 1131–1149.

Latif, M., and Coauthors, 2001: ENSIP: The El Niño Simulation Intercomparison Project. *Climate Dyn.,* **18,** 255–276.

Manabe, S., and R. T. Wetherald, 1967: Thermal equilibrium of the atmosphere with a given distribution of relative humidity. *J. Atmos. Sci.,* **24,** 241–259.

Ramanathan, V., and W. Collins, 1991: Thermodynamic regulation of ocean warming by cirrus clouds deduced from observations of the 1987 El Niño. *Nature,* **351,** 27–32.

Rossow, W. B., and R. A. Schiffer, 1999: Advances in understanding clouds from ISCCP. *Bull. Amer. Meteor. Soc.,* **80,** 2261–2288.

——, A. W. Walker, D. E. Beuschel, and M. D. Roiter, 1996: International Satellite Cloud Climatology Project (ISCCP) Documentation of New Cloud Datasets. WMO/TD-737, World Meteorological Organization, 115 pp.

Sun, D. Z., 2003: A possible effect of an increase in the warm-pool SST on the magnitude of El Niño warming. *J. Climate,* **16,** 185–205.

——, and R. S. Lindzen, 1993: Water vapor feedback and the ice age snowline record. *Ann. Geophys.,* **11,** 204–215.

——, and I. Held, 1996: A comparison of modeled and observed relationships between interannual variations of water vapor and temperature. *J. Climate,* **9,** 665–675.

——, and K. E. Trenberth, 1998: Coordinated heat removal from the equatorial Pacific during the 1986–87 El Niño. *Geophys. Res. Lett.,* **25,** 2659–2662.

Trenberth, K. E., 1997: Using atmospheric budgets as a constraint on surface fluxes. *J. Climate,* **10,** 2796–2809.

——, J. M. Caron, and D. P. Stepaniak, 2001: The atmospheric energy budget and implications for surface fluxes and ocean heat transports. *Climate Dyn.,* **17,** 259–276.

Zhang, G. J., and N. A. McFarlane, 1995: Sensitivity of climate simulations to the parameterization of cumulus convection in the Canadian Climate Centre general circulation model. *Atmos.–Ocean,* **33,** 407–446.